


SCIENTIFIC REPORTS



OPEN

The Th17/Treg Cytokine Imbalance in Chronic Obstructive Pulmonary Disease Exacerbation in an Animal Model of Cigarette Smoke Exposure and Lipopolysaccharide Challenge Association

Daniela A. B. Cervilha¹, Juliana T. Ito¹, Juliana D. Lourenço¹, Clarice R. Olivo^{1,2}, Beatriz M. Saraiva-Romanholo^{1,2}, Rildo A. Volpini³, Manoel C. Oliveira-Junior⁴, Thais Mauad⁵, Milton A. Martins¹, Iolanda F. L. C. Tibério¹, Rodolfo P. Vieira^{6,7,8}  & Fernanda D. T. Q. S. Lopes¹

We proposed an experimental model to verify the Th17/Treg cytokine imbalance in COPD exacerbation. Forty C57BL/6 mice were exposed to room air or cigarette smoke (CS) (12 ± 1 cigarettes, twice a day, 30 min/exposure and 5 days/week) and received saline (50 μ l) or lipopolysaccharide (LPS) (1 mg/kg in 50 μ l of saline) intratracheal instillations. We analyzed the mean linear intercept, epithelial thickness and inflammatory profiles of the bronchoalveolar lavage fluid and lungs. We evaluated macrophages, neutrophils, CD4⁺ and CD8⁺ T cells, Treg cells, and IL-10⁺ and IL-17⁺ cells, as well as STAT-3, STAT-5, phospho-STAT3 and phospho-STAT5 levels using immunohistochemistry and IL-17, IL-6, IL-10, INF- γ , CXCL1 and CXCL2 levels using ELISA. The study showed that CS exposure and LPS challenge increased the numbers of neutrophils, macrophages, and CD4⁺ and CD8⁺ T cells. Simultaneous exposure to CS/LPS intensified this response and lung parenchymal damage. The densities of Tregs and IL-17⁺ cells and levels of IL-17 and IL-6 were increased in both LPS groups, while IL-10 level was only increased in the Control/LPS group. The increased numbers of STAT-3, phospho-STAT3, STAT-5 and phospho-STAT5⁺ cells corroborated the increased numbers of IL-17⁺ and Treg cells. These findings point to simultaneous challenge with CS and LPS exacerbated the inflammatory response and induced diffuse structural changes in the alveolar parenchyma characterized by an increase in Th17 cytokine release. Although the Treg cell differentiation was observed, the lack of IL-10 expression and the decrease in the density of IL-10⁺ cells observed in the CS/LPS group suggest that a failure to release this cytokine plays a pivotal role in the exacerbated inflammatory response in this proposed model.

¹Department of Medicine, Laboratory of Experimental Therapeutics (LIM-20), School of Medicine, University of Sao Paulo, Sao Paulo, Brazil. ²Department of post-graduation of Institute of Medical Assistance to the State Public Servant, University City of Sao Paulo, Sao Paulo, Brazil. ³Nephrology Department, School of Medicine, University of Sao Paulo, Sao Paulo, Brazil. ⁴Laboratory of Pulmonary and Exercise Immunology, Nove de Julho University, Sao Paulo, Brazil. ⁵Department of Pathology, School of Medicine, University of Sao Paulo, Sao Paulo, Brazil. ⁶Post-graduation Program in Bioengineering and in Biomedical Engineering, Universidade Brasil, Sao Paulo, Brazil. ⁷Post-graduation Program in Sciences of Human Movement and Rehabilitation, Federal University of Sao Paulo (UNIFESP), Santos, Brazil. ⁸Brazilian Institute of Teaching and Research in Pulmonary and Exercise Immunology (IBEPIPE), Sao Jose dos Campos, Brazil. Correspondence and requests for materials should be addressed to D.A.B.C. (email: danielaapbrito@gmail.com)

Chronic obstructive pulmonary disease (COPD) is the fourth highest cause of mortality in the world, and it is predicted to become the third cause of death worldwide by 2020^{1,2}. The use of tobacco has been identified as a main risk factor for the development of this disease³.

After many years of smoking, the lungs become inflamed and exhibit the hypersecretion of mucus, providing a site for colonization of infectious pathogens⁴ that could culminate in the exacerbation of respiratory diseases^{5–10}. Clinical studies have identified a correlation between recurrent respiratory bacterial¹¹ or viral infections and COPD exacerbation^{10,12–14}, and the pivotal roles of innate and adaptive immune responses in the worsening of this lung disease^{15,16}.

Regarding the innate immune response, macrophages are part of the first line of lung defense in early events of infections induced by bacterial or viral agents. These cells phagocytose microbes and apoptotic cells to eliminate deleterious agents and also are responsible for releasing some pro-inflammatory mediators that promote neutrophil migration to the pulmonary site¹⁷. However, cigarette smoke (CS) exposure impairs macrophage activity¹⁷, and the persistence of this inflammatory process culminates in COPD progression^{15,17}.

COPD progression is associated with an infiltration of CD8⁺ and CD4⁺ T lymphocytes mainly into the small airways^{15,18}.

The effector immune responses result from the differentiation of naïve CD4⁺ T cells into Th1, or Th2, or Th17 or regulatory T cells (Treg) depending on the cytokines that signal through the Janus kinase (JAK) - signal transducer and activator of transcription (STAT) pathway^{19,20}.

Interleukin (IL)-6, IL-23 and tumor growth factor-beta (TGF- β) activate STAT3 and subsequently induce Th17 differentiation. In contrast, Treg differentiation depends on the presence of IL-12 and TGF- β to activate STAT5²¹.

Treg cells are recognized by their ability to suppress inflammation and to inhibit autoimmunity²². Anti-inflammatory cytokines such as IL-10 and TGF- β are also released by Treg cells^{23,24}. In our previous study, a decrease in the numbers of Treg cells and TGF- β ⁺ and IL-10⁺ cells was associated with an increase in the number of IL-17⁺ cells in the airways of smokers, leading to obstructions²⁵.

Although the importance of Treg cells in COPD progression has been described²⁵, the importance of this T cell subtype in COPD exacerbation remains unclear.

On the other hand, the Th17 response has been described both in COPD progression²⁶ and in bacterial infections in patients with COPD presenting exacerbations. Ross and colleagues²⁷ observed increased IL-17A levels in the bronchoalveolar lavage fluid (BALF) and lung tissues of patients with COPD, followed by neutrophil recruitment during acute exacerbations induced by a *Haemophilus influenzae* infection.

Lipopolysaccharide (LPS) is a pro-inflammatory component of gram-negative bacteria that is present in high amounts in CS^{28–30}. It has been extensively used in animal models to induce systemic inflammation and, depending on the dose, is capable of inducing pulmonary emphysema³¹.

Recently, LPS has been used in murine models to resemble COPD exacerbations in humans. Kobayashi and colleagues³² proposed a model of COPD exacerbation combining the instillation of elastase and LPS and verified an infiltration of CD8⁺ T cells into alveolar spaces and an increase in metalloproteinase-9 and perforin levels in the BALF. Additionally, Vernooij and colleagues³³ observed chronic lung inflammation characterized by the presence of lymphocytic aggregates in peribronchial and perivascular areas following long-term exposure to LPS.

Since tobacco smoking is the main etiological factor contributing to the development of COPD in humans and bacterial infections are known to induce an adaptive immune response resulting in the exacerbation of this disease, in this present study, we intend to verify the role of the adaptive immune response in COPD exacerbation using a CS exposure model treated with an LPS instillation, focusing on the Th17/Treg cytokine imbalance in this process.

Material and Methods

Animals. Forty male C57BL/6 mice (20–25 g), aged 6–8 weeks were used in this study. This study was performed using a protocol approved by the Ethics in Research Committee for Human and Animal Studies of University of São Paulo School of Medicine (São Paulo, Brazil) (protocol number 077/14). All animals received humane care in compliance with the Guide for the Care and Use of Laboratory Animals published by the US National Institutes of Health (NIH Publication N°. 85–23, revised 1996).

Experimental groups. Mice were either exposed to room air and received two instillations of a saline solution (Control/SAL) or LPS solution (Control/LPS), or were exposed to CS and received two instillations of a saline solution (CS/SAL) or LPS solution (CS/LPS) (Fig. 1).

Experimental protocol. Animals were exposed to CS or room air for 3 months. They received saline or LPS instillations on the 91st and 106th days. Animals were euthanized three days after the last instillation (Fig. 1).

Induction of emphysema. Animals were exposed to CS using methods previously described by Toledo and colleagues to induce COPD³⁴. We used a plastic box (28 L) with two inlets for synthetic air and smoke supplies. An airflow of 2 L/min was maintained and regulated by a flowmeter that passed through a Venturi System connected to a lit cigarette, providing the suction of CS into the box. A flow rate was set to produce carbon monoxide (CO) levels ranging from 250 to 350 ppm. Approximately 12 (\pm 1) commercially filtered cigarettes were used per day (0.8 mg of nicotine, 10 mg of tar and 10 mg of CO per cigarette), with a total particulate matter concentration of $354.8 \pm 50.3 \mu\text{g}/\text{m}^3/\text{day}$. The animals were housed in the smoke environment for 30 min/day, 2 times/day for 5 days/week for a period of 14 weeks. The control groups remained in room air (Fig. 1).

Intratracheal LPS challenge. The intratracheal challenge with LPS (*E. coli*, serotype O26:B6; Sigma Chemical Co.) was performed to simulate bacterial stimuli via an anterior cervical incision to expose the trachea.

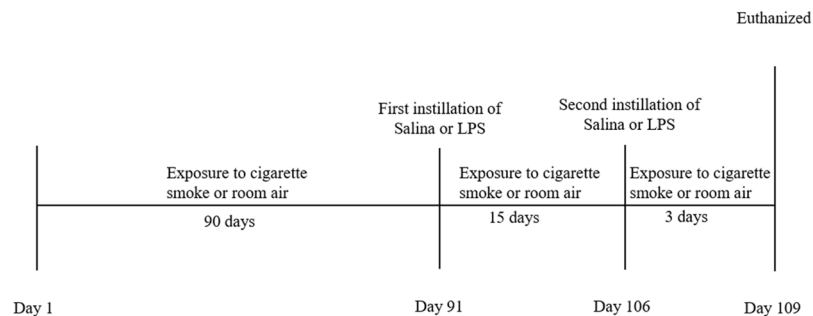


Figure 1. Timeline of the experimental protocol.

Animals received the LPS (1 mg/kg diluted in 50 μ l of a sterile saline solution) or sterile saline solution (0.9% NaCl; 50 μ l)³². Mice were placed on a heated animal bed (30 °C) until they showed active movements. They were also subjected to post-surgical recovery procedure and received tramadol chlorhydrate (5 mg/mL) via intramuscular injections (Fig. 1). Thus, we did not observe any considerable differences in animal's behavior. After the recovery period, animals were returned to the cage under normal conditions. The animals were active and did not display signs of post-operative pain.

Bronchoalveolar lavage fluid (BALF). At the end of the protocol, mice were intraperitoneally anaesthetized with thiopental (70 mg/kg) and euthanized by transecting the abdominal aorta. BALF was obtained through the tracheal cannula by washing the airway lumen with 3 \times 0.5 ml of sterile saline. BALF samples were centrifuged at 1000 rpm at 4 °C for 10 min and the cell pellet was resuspended in 0.2 mL of sterile saline for the Control groups and 1.5 mL of sterile saline for LPS groups. Total cell numbers were determined using a Neubauer hemocytometer counting chamber (Carl Roth, Karlsruhe, Germany). Differential cell counts were evaluated by a microscopic examination of BALF samples prepared on cytocentrifuge slides that were stained with Diff Quick (Medion Diagnostics, Dündingen, Switzerland)³⁵.

Lung preparation. Lungs were removed en bloc and fixed with 4% formaldehyde infused through the trachea at constant pressure of 20 cmH₂O for 24 h. Lungs were embedded in paraffin and cut into 5 μ m coronal sections.

Morphometry. For conventional morphometry, we used an eyepiece with a coherent system of 50 lines and 100 points with a known area attached to the microscope ocular to perform the mean linear intercept (Lm) measurements, an indicator of the mean alveolar diameter³⁶. Tissue samples were stained with hematoxylin and eosin (H&E). For each animal, images of 20 fields at a magnification of 200 \times were captured. Lm was obtained by counting the number of times that the lines of the reticulum intercepted the alveolar walls and calculated using the following equation: $Lm = Ltotal/Nl$.

We performed the Lm analysis in subpleural airspaces and peribronchial airspaces.

Epithelial thickness. Histological sections were stained with H&E to evaluate the epithelial thickness. We used the Panoramic Viewer 1.5 (3DHISTECH, Budapest, Hungary), an image analysis system. We quantified 5 airways from each animal at a magnification of 400 \times . Epithelial thickness was defined as the distance between the basement membrane and the luminal cell membrane, excluding the cilia³⁷, and the length of basement membrane was determined. The epithelial thickness was expressed as a relationship between the epithelial thickness and the length of basement membrane.

Immunohistochemistry. Tissue sections were deparaffinized and hydrated. After blocking endogenous peroxidase activity, antigen retrieval was performed with a high-temperature citrate buffer (pH = 6.0). The primary antibodies used in this study were: a rat monoclonal antibody against Mac-2 (1:50000, Cedarlane, Ontario, CA), a rabbit polyclonal antibody against neutrophil elastase (1:2000, Abcam, Cambridge, UK), a rabbit polyclonal antibody against FOXP3 (1:500, Abcam, Cambridge, UK), a rat monoclonal antibody against CD4 (1:10, Santa Cruz, CA, USA), a rabbit polyclonal antibody against CD8 (1:100, Abcam, Cambridge, UK), a rabbit polyclonal antibody against IL-17 (1:200, Abcam, Cambridge, UK), and a rat monoclonal antibody against IL-10 (1:30, Santa Cruz, CA, USA), a rabbit polyclonal antibody against STAT3 (1:1000, Santa Cruz, CA, USA), a goat polyclonal antibody against phospho-STAT3 (1:2000, Santa Cruz, CA, USA), a goat polyclonal antibody against STAT5 (1:2000, Santa Cruz, CA, USA), and a goat polyclonal antibody against phospho-STAT5 (1:100, Santa Cruz, CA, USA). The Vectastain ABC Kit (Vector Laboratories, Burlingame, CA, USA) was used in conjunction with a species-specific secondary antibody or Histofine Polymer (Nichirei Biosciences, Tokyo, JP), and the sections were stained using chromogen diaminobenzidine (DAB, Sigma, St. Louis, MO, USA). Sections were counterstained with Harris hematoxylin (Merck, Darmstadt, Germany). For negative controls, the primary antibody was omitted³⁴ and replaced with BSA for the incubation with tissue sections.

Images of the lung tissues were captured from 15–20 random parenchymal fields for each lung sample at 400 \times magnification using the Panoramic Viewer 1.5 (3DHISTECH, Budapest, Hungary). We used a digital analysis system and specific software (Image-Pro Plus version 4.5 for Windows, Media Cybernetics, MD, USA) to determine the area of pulmonary parenchyma. Then, we quantified the density of positive cells for Mac-2, neutrophil

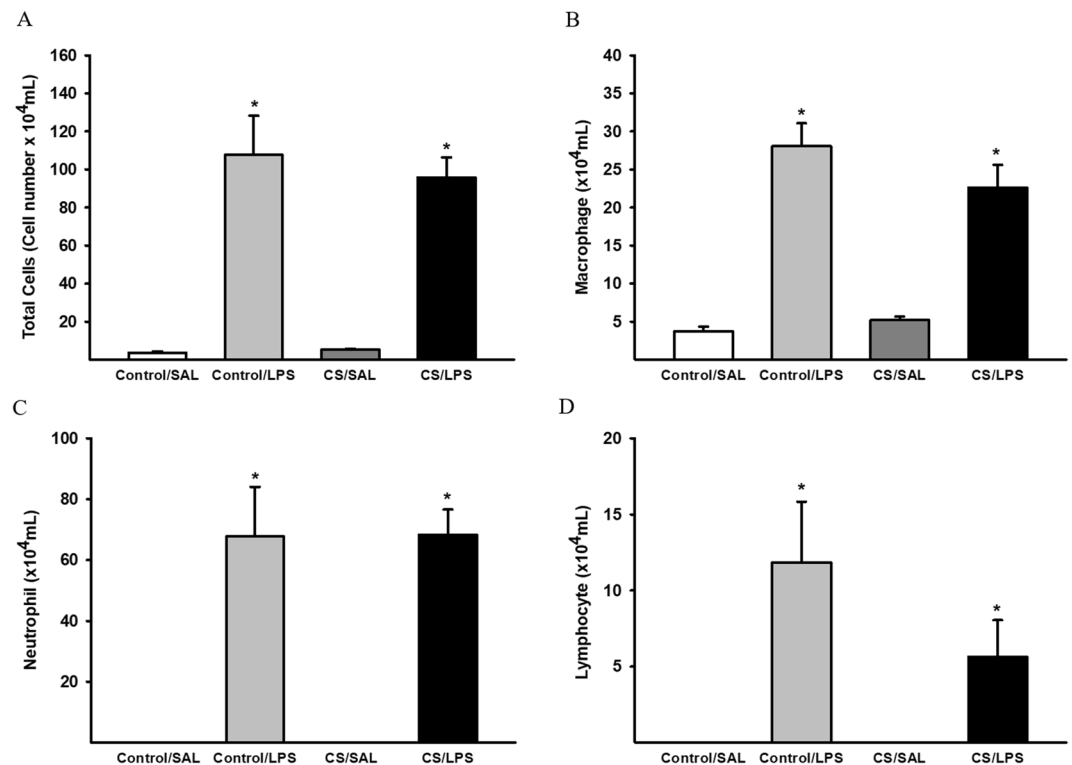


Figure 2. Inflammatory cells in the BAL. **(A)** Total cells, * $p < 0.001$ compared to Control/SAL and CS/SAL; Control/SAL $n = 10$, Control/LPS $n = 6$, CS/SAL $n = 9$, CS/LPS $n = 7$. ANOVA, Holm-Sidak post hoc. **(B)** Macrophages, * $p < 0.001$ compared to Control/SAL and CS/SAL; Control/SAL $n = 10$, Control/LPS $n = 7$, CS/SAL $n = 6$, CS/LPS $n = 7$. **(C)** Neutrophils, * $p < 0.001$ compared to Control/SAL and CS/SAL; Control/SAL $n = 10$, Control/LPS $n = 6$, CS/SAL $n = 7$, CS/LPS $n = 7$. **(D)** Lymphocyte, * $p < 0.001$ compared to Control/SAL and CS/SAL. Control/SAL $n = 10$, Control/LPS $n = 4$, CS/SAL $n = 7$, CS/LPS $n = 7$. Kruskal-Wallis, Dunn's post hoc. Data are presented as means and SE.

elastase, CD4, CD8, FOXP3, IL-10, IL-17, STAT3, phospho-STAT3, STAT5 and phospho-STAT5 per parenchymal area, which was reported as cells/ μm^2 .

Double immunohistochemical staining. We performed double immunostaining to examine the deficiency in IL-10 expression in Treg cells. Firstly, lung tissue sections were stained with a rabbit polyclonal against FOXP3 (1:300, Abcam, Cambridge, UK) using an immunoperoxidase procedure and DAB as chromogen. Afterwards, sections were incubated with a rat monoclonal antibody against IL-10 (1:100, Santa Cruz, CA, USA) using an equivalent protocol with an immunoalkaline phosphatase procedure and a red colored reaction product (PermaRed/AP, Diagnostic BioSystems, Pleasanton, CA). Finally, Harris hematoxylin was used to counterstain tissue sections. Images of the lung tissues were captured with an AxioCam digital camera MRC5 using the software Zen from Carl Zeiss (München-Hallbergmoos, Germany). We captured images at magnifications of 400 \times and 1000 \times .

Cytokine analysis. Lungs were homogenized in a saline solution (0.9% NaCl), centrifuged, and the supernatants were stored at -80°C until subsequent analyses. The levels of IL-17, interferon-gamma (IFN- γ), chemokine C-X-C motif ligand 1 (CXCL1) and CXCL2 were quantified using enzyme linked immunosorbent assays (ELISA). The kits were purchased from R&D System (Minneapolis, MN), and the levels of IL-6 and IL-10 were quantified using ELISA kits purchased from BioLegend (San Diego, CA). The ELISA was performed according to the manufacturers' instructions.

Statistical analysis. The statistical analysis was performed using SigmaStat statistical software (Systat Software, San Jose, CA). For immunohistochemistry and cytokine analyses, we logarithmically transformed the data. Data were analyzed using one-way ANOVA followed by Holm-Sidak post hoc analysis for data with a parametric distribution or Kruskal-Wallis test for data with a nonparametric distribution and Dunn's post hoc analysis. Results are presented as means \pm SE and p value < 0.05 was considered statically significant.

Ethical approval. This study was performed under a protocol approved by the Ethics in Research Committee for human and animal studies of University of São Paulo School of Medicine (São Paulo, Brazil) (protocol number 077/14). All animals received humane care in compliance with the Guide for the Care and Use of Laboratory Animals published by the US National Institutes of Health (NIH Publication N $^\circ$. 85-23, revised 1996).

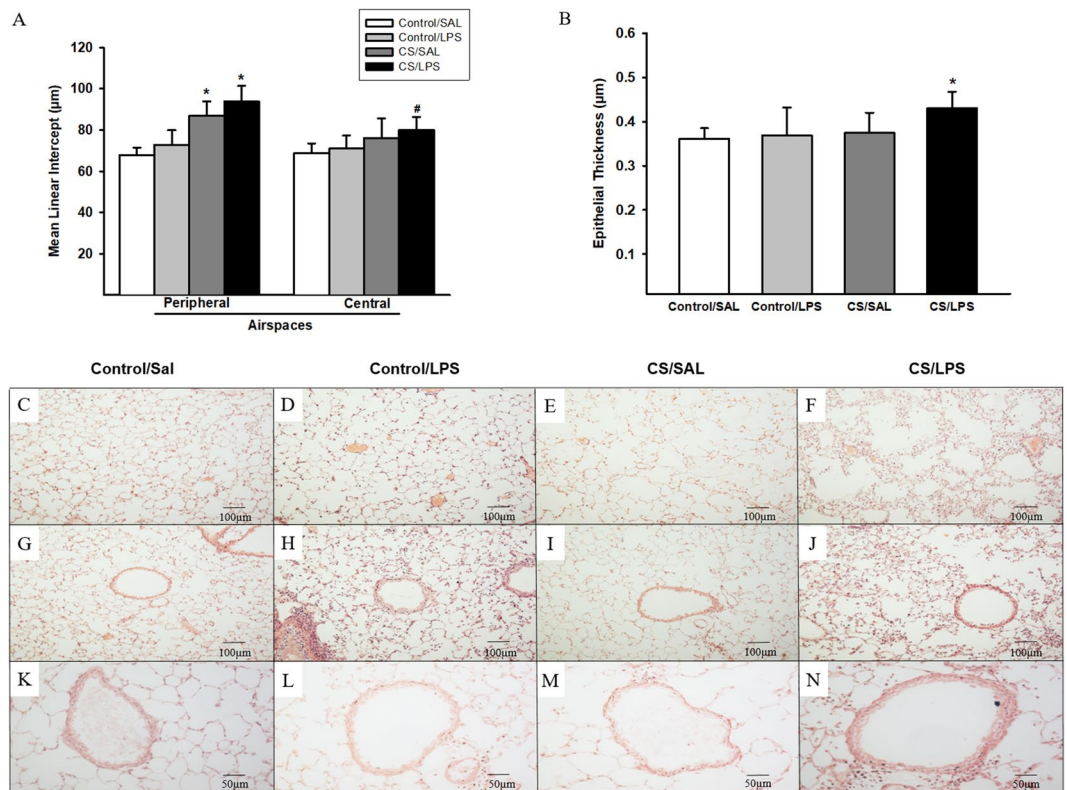


Figure 3. Mean linear intercept measured in subpleural airspaces and peribronchial airspaces and epithelial thickness in the experimental groups. (A) Lm: * $p < 0.001$ compared to Control/SAL and Control/LPS groups. Control/SAL $n = 9$, Control/LPS $n = 9$, CS/SAL $n = 8$, CS/LPS $n = 5$. ANOVA, Holm-Sidak post hoc. # $p = 0.02$ compared to Control/SAL. Control/SAL $n = 9$, Control/LPS $n = 9$, CS/SAL $n = 8$, CS/LPS $n = 5$. Kruskal-Wallis, Dunn's post hoc. Photomicrographs of Lm in subpleural airspaces and peribronchial airspaces. (C,G) Control/SAL group; (D,H) Control/LPS group; (E,I) CS/SAL group and (F,J) CS/LPS group, respectively, 200X magnification. (B) Epithelial thickness: * $p = 0.02$ compared to Control/SAL. Control/SAL $n = 9$, Control/LPS $n = 9$, CS/SAL $n = 8$, CS/LPS $n = 5$. ANOVA, Holm-Sidak post hoc. Photomicrographs of epithelial thickness in airways (K) Control/SAL group; (L) Control/LPS group; (M) CS/SAL group and (N) CS/LPS group. Data are presented as means and SE. 400X magnification.

Results

Inflammatory changes in BALF. The intratracheal instillation of LPS induced a significant increase in the numbers of total cells, macrophages, neutrophils and lymphocytes in the BALF compared to the Control/SAL and CS/SAL groups (Fig. 2A–D).

Lung morphometry. Alveolar enlargement was observed in the subpleural airspaces of animals exposed to CS compared to Control groups. However, we only observed alveolar enlargement in the peribronchial airspaces in the CS/LPS group, but not the Control/SAL group (Fig. 3A,C–J).

An increase in epithelial thickness was observed in the CS/LPS group compared to the Control/SAL group (Fig. 3B,K–N).

Lung tissue inflammation. We observed increased densities of macrophages and neutrophils in the lung parenchyma of animals that were challenged with LPS compared to the Control/SAL and CS/SAL. We also observed an increase in the densities of these cells in the CS/LPS group compared to the Control/LPS group. Furthermore, we observed an increase in the CS/SAL group compared to the Control/SAL group (Fig. 4A–J, respectively).

The groups that received LPS challenge showed increased densities of CD4⁺ and CD8⁺ T cells compared to the Control/SAL group (Figs 4K–O and 5A–E, respectively). We also identified an increase in the CS/SAL group compared to the Control/SAL group. In addition, we observed an increase in the density of CD4⁺ cells in the CS/LPS group compared to the CS/SAL and Control/LPS groups (Fig. 4K–O).

The LPS challenge (Control/LPS and CS/LPS) increased the density of FOXP3⁺ cells compared to Control/SAL group (Fig. 6A–E). The density of STAT3⁺ cells was increased in the lung parenchyma of animals challenged with LPS compared to the Control/SAL and CS/SAL groups. We also observed an increase in the CS/LPS group compared to the Control/LPS group. Furthermore, we observed an increase in the CS/SAL group compared to Control/SAL group (Fig. 5F–J). Moreover, the LPS challenge (Control/LPS and CS/LPS) increased the density

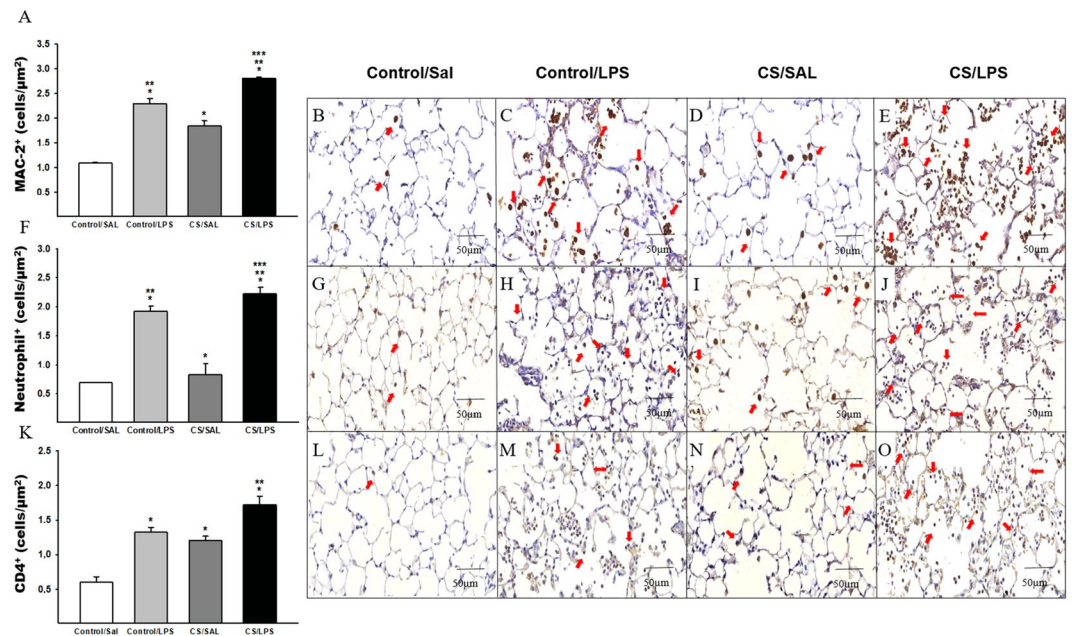


Figure 4. The density of positive cells for MAC-2, neutrophils and CD4⁺ in experimental groups. **(A)** MAC-2: * $p < 0.001$ compared to Control/SAL; ** $p < 0.001$ compared to CS/SAL group and *** $p < 0.001$ compared to Control/LPS group. Control/SAL $n = 9$, Control/LPS $n = 9$, CS/SAL $n = 7$, CS/LPS $n = 5$. Photomicrographs of MAC-2 in lung parenchyma **(B)** Control/SAL group; **(C)** Control/LPS group; **(D)** CS/SAL group and **(E)** CS/LPS group, 400X magnification. **(F)** Neutrophils: * $p < 0.001$ compared to Control/SAL; ** $p < 0.001$ compared to CS/SAL group and *** $p < 0.001$ compared to Control/LPS group. Control/SAL $n = 9$, Control/LPS $n = 9$, CS/SAL $n = 8$, CS/LPS $n = 5$. Photomicrographs of neutrophils in lung parenchyma **(G)** Control/SAL group; **(H)** Control/LPS group; **(I)** CS/SAL group and **(J)** CS/LPS group, 400X magnification. **(K)** CD4⁺: * $p < 0.001$ compared to Control/SAL. ** $p < 0.001$ compared to CS/SAL and Control/LPS groups. Control/SAL $n = 9$, Control/LPS $n = 9$, CS/SAL $n = 8$, CS/LPS $n = 5$. Photomicrographs of CD4 T cells in lung parenchyma **(L)** Control/SAL group; **(M)** Control/LPS group; **(N)** CS/SAL group and **(O)** CS/LPS group, 400X magnification. Data were expressed as log₁₀ base. ANOVA, Holm-Sidak post hoc. Data are presented as means and SE.

of phospho-STAT3⁺ cells compared to the Control/SAL group (Fig. 5K–O). We observed an increase in the density of STAT5⁺ cells in the Control/LPS group compared to the Control/SAL and CS/SAL groups (Fig. 6F–J). In addition, we detected an increase in the density of phospho-STAT5⁺ cells in the lung parenchyma of animals challenged with LPS compared to the Control/SAL and CS/SAL groups, and we observed an increase in the CS/LPS group compared to the Control/LPS group (Fig. 6K–O).

The density of IL-10⁺ cells was increased in the lung parenchyma of animals challenged with LPS compared to the Control/SAL group. We also observed an increase in the Control/LPS group compared to the CS/SAL and CS/LPS groups (Fig. 7A–E). Moreover, the LPS challenge (Control/LPS and CS/LPS) increased the density of IL-17⁺ cells compared to the Control/SAL group (Fig. 7F–J).

Regarding the ratio of normalized phosphoSTAT3/STAT3, there were no significant differences among the experimental groups. However, the ratio of phosphoSTAT5/STAT5 was increased in the CS/LPS compared to the Control/SAL and CS/SAL groups (Fig. 8A,B, respectively).

Measurement of cytokine levels in lung homogenates. The LPS challenge significantly increased IL-17 and IL-6 levels compared to the Control/SAL group (Fig. 9A,B, respectively). In Control/LPS and CS/LPS groups, we also detected increased levels of the CXCL1 and CXCL2 chemokines compared to the Control/SAL and CS/SAL groups. In addition, an increase in CXCL1 levels was detected in the CS/SAL group compared to the Control/SAL group and an increase in CXCL2 levels in the CS/LPS group compared to the Control/LPS group (Fig. 9C,D, respectively). The IL-10 levels were increased in the Control/LPS group compared to the Control/SAL and CS/SAL groups (Fig. 9E). We did not observe significant differences in INF- γ levels among the groups (Fig. 9F).

Double Staining for Treg and IL-10. The analysis of Treg/IL-10-positive cells revealed an increase in the Control/LPS group compared to the CS/LPS group (Fig. 10A,B, respectively).

Discussion

CS exposure and subsequent LPS challenge induced an inflammatory process in the BALF and lung parenchyma similar to the process observed in patients with COPD presenting an exacerbation^{8,38,39}. Moreover, this dual CS/LPS challenge increased the epithelial thickness and resulted in diffuse alveolar enlargement in the peribronchial and subpleural airspaces, reflecting a noticeable injury to the parenchymal architecture.

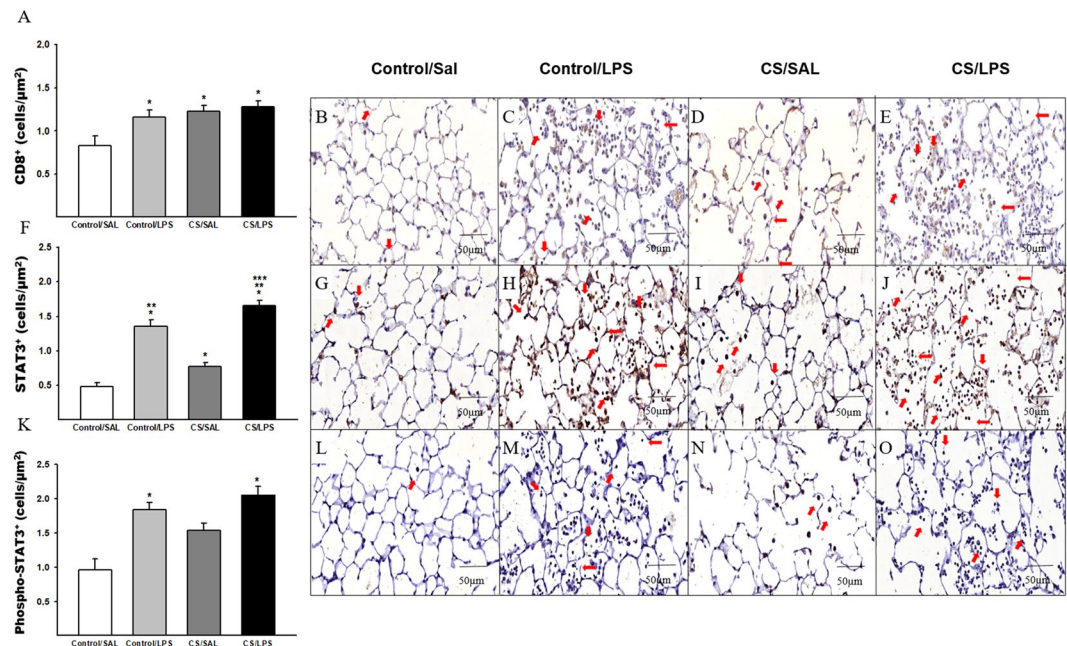


Figure 5. The density of positive cells for CD8⁺, STAT3 and Phospho-STAT3 in experimental groups. (A) CD8⁺: **p* = 0.006 compared to Control/SAL. Control/SAL *n* = 9, Control/LPS *n* = 9, CS/SAL *n* = 8, CS/LPS *n* = 5. Photomicrographs of CD8 T cells in lung parenchyma (B) Control/SAL group; (C) Control/LPS group; (D) CS/SAL group and (E) CS/LPS group, 400X magnification. (F) STAT3: **p* < 0.001 compared to Control/SAL; ***p* < 0.001 compared to CS/SAL group and ****p* < 0.001 compared to Control/LPS group. Control/SAL *n* = 7, Control/LPS *n* = 9, CS/SAL *n* = 6, CS/LPS *n* = 5. Photomicrographs of STAT3 in lung parenchyma (G) Control/SAL group; (H) Control/LPS group; (I) CS/SAL group and (J) CS/LPS group, 400X magnification. Data were expressed as log₁₀ base. ANOVA, Holm-Sidak post hoc. Data are presented as means and SE. (K) Phospho-STAT3: **p* < 0.001 compared to Control/SAL. Control/SAL *n* = 8, Control/LPS *n* = 8, CS/SAL *n* = 8, CS/LPS *n* = 4. Photomicrographs of Phospho-STAT3 in lung parenchyma (L) Control/SAL group; (M) Control/LPS group; (N) CS/SAL group and (O) CS/LPS group, 400X magnification. Data were expressed as log₁₀ base. Kruskal-Wallis, Dunn's post hoc. Data are presented as means and SE.

LPS alone increased the densities of both IL-17⁺ cells and Treg cells, but did not increase IL-10 levels in the CS/LPS group. LPS alone also decreased the number of IL-10⁺ cells in this group compared to the Control/LPS group. Therefore, we suggest that decreased IL-10 production plays a pivotal role in the inflammatory exacerbation in this proposed model.

We observed an inflammatory process in the lung parenchyma of CS groups that was mainly characterized by increased numbers of macrophages, neutrophils, CD4⁺ and CD8⁺ T cells, and the subsequent LPS challenge intensified this response. The BALF analysis only revealed statistically significant increases in the numbers of macrophages and total cells in LPS groups. Since the BALF analysis include airways other than the parenchymal areas, an intensified inflammatory response that mainly occurred in parenchymal areas was observed in this animal model.

Alveolar macrophages are known to recruit other cell types to the site of inflammation by releasing chemokines⁴⁰; for example, CXCL1 (chemokine homologous to IL-8) and CXCL2⁴¹ that are chemoattractants for neutrophils⁴². These findings are in consistent with the higher expression of CXCL1 and CXCL2 in lung homogenates observed in our study.

While CXCL1 expression was increased by exposure to CS or LPS challenge, the levels of CXCL2 were increased only in LPS groups, and the CS/LPS challenge exacerbated this response. Moreover, the administration of both stimuli further increased the neutrophil density in parenchyma, which reinforces the importance of innate immune response in this experimental model¹⁶.

In patients with COPD, the exacerbation due to bacterial colonization is mainly mediated by IL-8 released by neutrophils⁴³, and both neutrophils and IL-8 production are associated with an increase in sputum production and worsening airway obstruction^{44–46}.

Regarding T cell subtypes, we observed increased numbers of CD8⁺ and CD4⁺ T cells in both LPS and CS groups, consistent with previous studies using animal models of COPD^{31,32,47}; however, we reported a greater increase in the number of CD4⁺ T cells in animals exposed to CS/LPS. The number of CD8⁺ T cells is increased in the respiratory tract and in the parenchyma of smokers with COPD⁴⁸, and the activation of these cells might contribute to COPD progression⁴⁹.

We analyzed the density of positive cells for STAT3 and phospho-STAT3 and STAT5 and phospho-STAT5 to evaluate the balance between Th17 and Treg differentiation.

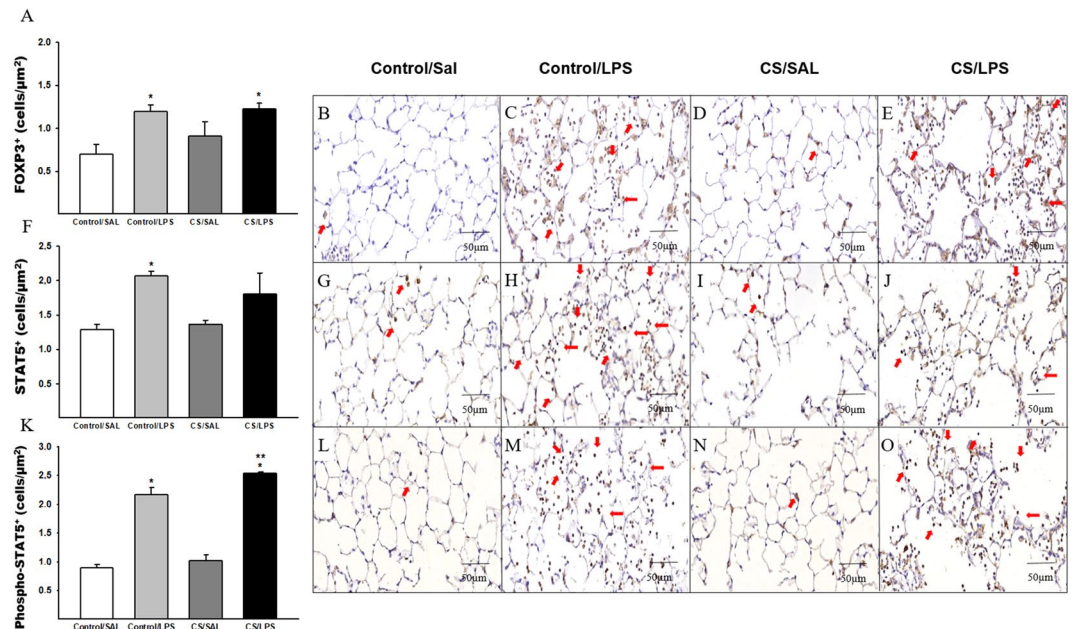


Figure 6. The density of positive cells for FOXP3, STAT5 and Phospho-STAT5 in experimental groups. **(A)** FOXP3: * $p = 0.01$ compared to Control/SAL. Control/SAL $n = 9$, Control/LPS $n = 9$, CS/SAL $n = 8$, CS/LPS $n = 5$. Photomicrographs of FOXP3 cells in lung parenchyma **(B)** Control/SAL group; **(C)** Control/LPS group; **(D)** CS/SAL group and **(E)** CS/LPS group, respectively, 400X magnification. Data were expressed as \log_{10} base. ANOVA, Holm-Sidak post hoc. Data are presented as means and SE. **(F)** STAT5: * $p < 0.001$ compared to Control/SAL and CS/SAL groups. Control/SAL $n = 9$, Control/LPS $n = 9$, CS/SAL $n = 8$, CS/LPS $n = 5$. Photomicrographs of STAT5 in lung parenchyma **(G)** Control/SAL group; **(H)** Control/LPS group; **(I)** CS/SAL group and **(J)** CS/LPS group, 400X magnification. Data were expressed as \log_{10} base. Kruskal-Wallis, Dunn's post hoc. Data are presented as means and SE. **(K)** Phospho-STAT5: * $p < 0.001$ compared to Control/SAL and CS/SAL groups; ** $p < 0.001$ compared to Control/LPS group. Control/SAL $n = 9$, Control/LPS $n = 9$, CS/SAL $n = 8$, CS/LPS $n = 5$. Photomicrographs of Phospho-STAT5 in lung parenchyma **(L)** Control/SAL group; **(M)** Control/LPS group; **(N)** CS/SAL group and **(O)** CS/LPS group, 400X magnification. Data were expressed as \log_{10} base. ANOVA, Holm-Sidak post hoc. Data are presented as means and SE.

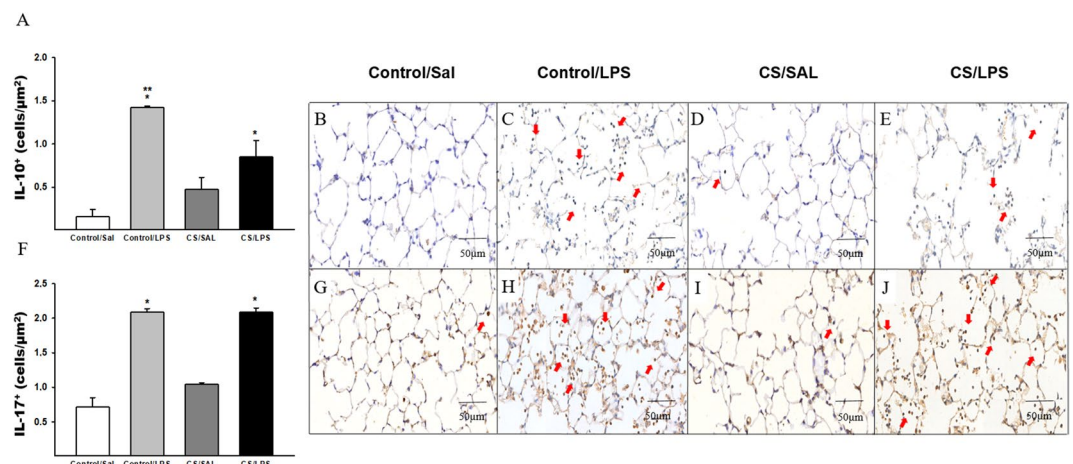


Figure 7. The density of positive cells for IL-10 and IL-17 in experimental groups. **(A)** IL-10: * $p = 0.001$ compared to Control/SAL; ** $p = 0.001$ compared to CS/SAL and CS/LPS. Control/SAL $n = 6$, Control/LPS $n = 6$, CS/SAL $n = 6$, CS/LPS $n = 5$. Photomicrographs of IL-10 cells in lung parenchyma **(B)** Control/SAL group; **(C)** Control/LPS group; **(D)** CS/SAL group and **(E)** CS/LPS group, 400X magnification. Data were expressed as \log_{10} base. ANOVA, Holm-Sidak post hoc. Data are presented as means and SE. **(F)** IL-17: * $p < 0.001$ compared to Control/SAL group. Control/SAL $n = 6$, Control/LPS $n = 6$, CS/SAL $n = 6$, CS/LPS $n = 5$. Photomicrographs of IL-17 in lung parenchyma **(G)** Control/SAL group; **(H)** Control/LPS group; **(I)** CS/SAL group and **(J)** CS/LPS group, 400X magnification. Data were expressed as \log_{10} base. Kruskal-Wallis, Dunn's post hoc. Data are presented as means and SE.

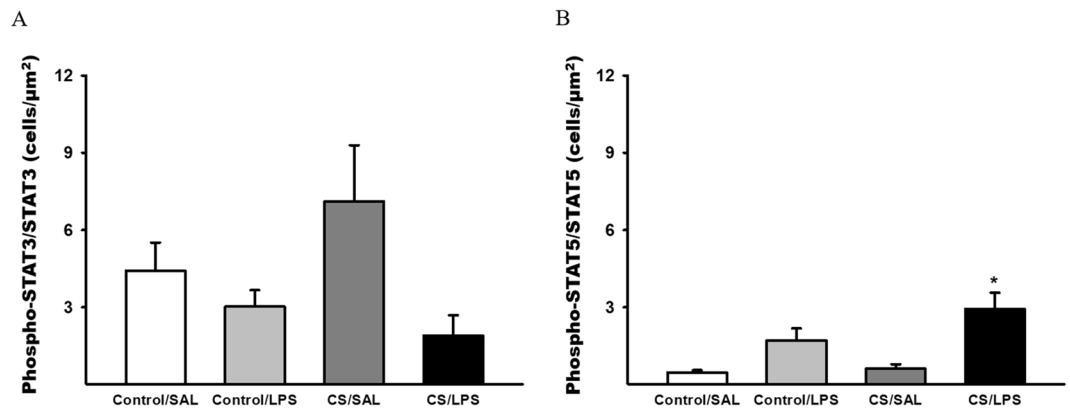


Figure 8. The ratio of normalized of PhosphoStat3/Stat3 and PhosphoStat5/Stat5. **(A)** PhosphoStat3/Stat3, there were no significant differences in parameters values among the experimental groups. Control/SAL $n = 7$, Control/LPS $n = 8$, CS/SAL $n = 6$, CS/LPS $n = 3$. **(B)** PhosphoStat5/Stat5, $*p = 0.002$ compared to Control/SAL. Control/SAL $n = 9$, Control/LPS $n = 9$, CS/SAL $n = 8$, CS/LPS $n = 4$. Kruskal-Wallis, Dunn's post hoc. Data were expressed as \log_{10} base. Data are presented as means and SE.

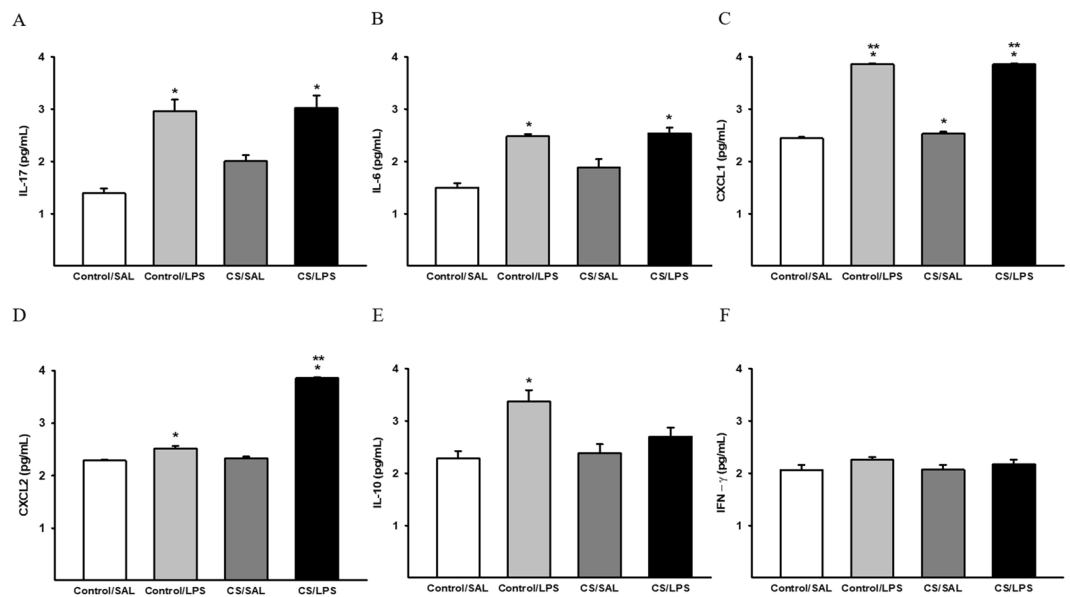


Figure 9. Cytokines and chemokines in lung homogenates. **(A)** IL-17: $*p < 0.001$ compared to Control/SAL. Control/SAL $n = 10$, Control/LPS $n = 6$, CS/SAL $n = 8$, CS/LPS $n = 7$. Kruskal-Wallis, Dunn's post hoc. **(B)** IL-6: $*p < 0.001$ compared to Control/SAL. Control/SAL $n = 10$, Control/LPS $n = 6$, CS/SAL $n = 9$, CS/LPS $n = 7$. Kruskal-Wallis, Dunn's post hoc. **(C)** CXCL1: $*p < 0.001$ compared to Control/SAL and $**p < 0.001$ compared to CS/SAL. Control/SAL $n = 10$, Control/LPS $n = 6$, CS/SAL $n = 9$, CS/LPS $n = 7$. ANOVA, Holm-Sidak post hoc. **(D)** CXCL2: $*p < 0.001$ compared to Control/SAL and CS/SAL and $**p < 0.001$ compared to Control/LPS group. Control/SAL $n = 10$, Control/LPS $n = 6$, CS/SAL $n = 9$, CS/LPS $n = 7$. ANOVA, Holm-Sidak post hoc. **(E)** IL-10: $*p < 0.01$ compared to Control/SAL and CS/SAL. Control/SAL $n = 10$, Control/LPS $n = 5$, CS/SAL $n = 7$, CS/LPS $n = 7$. Kruskal-Wallis, Dunn's post hoc. **(F)** IFN- γ : there were no significant differences in parameters values among the experimental groups. Control/SAL $n = 10$, Control/LPS $n = 6$, CS/SAL $n = 9$, CS/LPS $n = 7$. Kruskal-Wallis, Dunn's post hoc. Data were expressed as \log_{10} base. Data are presented as means and SE.

Both LPS and CS exposure increased the density of STAT3⁺ cells, and the administration of the combination of CS and LPS exacerbated this increase, corroborating the increase in IL-17 levels and the number of IL17⁺ cells in the lung. Di Stefano and colleagues⁵⁰ showed increased levels of IL-17A and IL-22 in bronchial mucosal biopsies from patients with stable COPD. In addition, Zhang and colleagues⁵¹ observed a significant increase in the number of CD4⁺IL17⁺ cells in the alveolar wall of patients with COPD that positively correlated with airway obstruction.

The increase in the number of STAT3⁺ cells is consistent with the increased IL-6 levels in both groups challenged with LPS, since IL-6 is recognized to switch Treg cells to a Th17 response following chronic infection⁵².

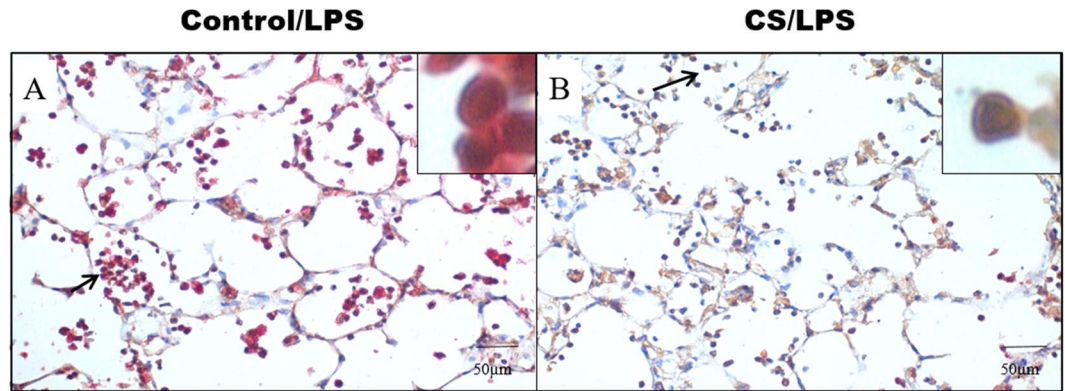


Figure 10. Representative photomicrographs of double immunostaining for FOXP3 (brown reaction product), IL-10 (red reaction product). FOXP3 positive cells was increased in parenchymal areas of CS/LPS while the co-localization of FOXP3/IL-10 (arrow) was found increased in Control/LPS group. (A) Control/LPS group and (B) CS/LPS group. 400X and 1000X magnification.

On the other hand, the density of phosphoSTAT3⁺ cells was increased in both groups that received LPS, and the administration of CS did not exacerbate this response. Moreover, the numbers of phosphoSTAT3⁺ cells/STAT3⁺ cells were decreased in the CS/LPS group, which was inconsistent with the increased IL-6 and IL-17 levels. Yew-Booth⁵³ and colleagues have previously described an increase in STAT3 levels, but not phosphoSTAT3 levels, in patients with COPD compared to smokers using immunohistochemistry, whereas when the authors analyzed the levels of these cytokines using western blotting, they detected increased levels of both STAT3 and phosphoSTAT3. The authors suggested that the antibody used in the study was more suitable for western blotting than for immunohistochemistry. Although we did not use the same antibody described by Yew-Booth and colleagues⁵³, our results are consistent with the previous findings described above, reinforcing the hypothesis that the immunohistochemistry might not be the best technique to evaluate STAT-3 phosphorylation.

Interestingly, we also observed an increase in the density of STAT5⁺ and phospho-STAT5⁺ cells in the LPS groups, and the higher values for phospho-STAT5⁺ cells were observed in the CS/LPS group, corroborating the increased density of Treg cells and the increased numbers of phosphoSTAT5⁺ cells/STAT5⁺ cells.

Nonetheless, the increase in Treg cells does not reflect an increase in IL-10 release⁵⁴. In the present study, although we observed an increase in the number of Treg cells in both groups that received the LPS instillation, only the Control/LPS group showed concomitantly increased IL-10 levels and IL-10⁺ cells density compared to the other experimental groups.

The increased numbers of other cell types, such as macrophages and neutrophils, in CS/LPS groups that are mediated by the release of this anti-inflammatory interleukin⁵⁵ are insufficient to induce an increase in IL-10 levels.

In the majority of infections, the IL-10 is an essential regulator to control the inflammatory response, and has a more important role than any other cytokine⁵⁵. In viral infections, the IL-10 produced by Treg cells is closely related to the maintenance of the immunopathological balance^{56–59}. Nevertheless, the inhibition of IL-10 signaling may exacerbate a pro-inflammatory response that clears pathogens but damages the lung tissue⁶⁰. Jin and colleagues⁶¹ previously reported similar results in serum from patients with COPD collected during an exacerbation to our findings. The authors showed an increase in IL-17 levels compared to healthy nonsmokers and patients with stable COPD, with a concomitant increase in the number of Treg/CD4⁺ cells. Therefore, although the Tregs are upregulated during acute exacerbations, their generation and differentiation were not sufficient, suggesting that both pro-inflammatory and anti-inflammatory reactions are enhanced, with pro-inflammatory and anti-inflammatory reactions enhanced, with pro-inflammatory reactions predominating during acute exacerbations in patients with COPD. Additionally, the authors showed normal Treg/IL-17 numbers; however, the Treg cells were not sufficient to suppress the exacerbated inflammatory process. In the present study, we did not evaluate how Treg function impaired IL-10 release. However, we showed the role of the TH17/Treg cytokine imbalance, highlighting the importance of a lack of IL-10 release in this COPD exacerbation model.

Conclusions

We showed that the Th17/Treg cytokine imbalance lead the inflammatory process exacerbation as well as the diffuse structural changes in lungs in this COPD exacerbation model.

Data Availability

The datasets generated during and/or analyzed during the current study are available from the corresponding author on reasonable request.

References

- Lozano, R. *et al.* Global and regional mortality from 235 causes of death for 20 age groups in 1990 and 2010: a systematic analysis for the Global Burden of Disease Study 2010. *Lancet* **380**, 2095–2128, [https://doi.org/10.1016/S0140-6736\(12\)61728-0](https://doi.org/10.1016/S0140-6736(12)61728-0) (2012).
- Mathers, C. D. & Loncar, D. Projections of global mortality and burden of disease from 2002 to 2030. *PLoS medicine* **3**, e442, <https://doi.org/10.1371/journal.pmed.0030442> (2006).

3. Silverman, E. K. & Speizer, F. E. Risk factors for the development of chronic obstructive pulmonary disease. *The Medical clinics of North America* **80**, 501–522 (1996).
4. Taylor, J. D. COPD and the response of the lung to tobacco smoke exposure. *Pulmonary pharmacology & therapeutics* **23**, 376–383, <https://doi.org/10.1016/j.pupt.2010.04.003> (2010).
5. Patel, I. S. *et al.* Relationship between bacterial colonisation and the frequency, character, and severity of COPD exacerbations. *Thorax* **57**, 759–764 (2002).
6. Seemungal, T. *et al.* Respiratory viruses, symptoms, and inflammatory markers in acute exacerbations and stable chronic obstructive pulmonary disease. *American journal of respiratory and critical care medicine* **164**, 1618–1623, <https://doi.org/10.1164/ajrccm.164.9.2105011> (2001).
7. Bhowmik, A., Seemungal, T. A., Sapsford, R. J. & Wedzicha, J. A. Relation of sputum inflammatory markers to symptoms and lung function changes in COPD exacerbations. *Thorax* **55**, 114–120 (2000).
8. Crooks, S. W., Bayley, D. L., Hill, S. L. & Stockley, R. A. Bronchial inflammation in acute bacterial exacerbations of chronic bronchitis: the role of leukotriene B4. *The European respiratory journal* **15**, 274–280 (2000).
9. Saetta, M. *et al.* Airway eosinophilia in chronic bronchitis during exacerbations. *American journal of respiratory and critical care medicine* **150**, 1646–1652, <https://doi.org/10.1164/ajrccm.150.6.7952628> (1994).
10. Donaldson, G. C., Seemungal, T. A., Bhowmik, A. & Wedzicha, J. A. Relationship between exacerbation frequency and lung function decline in chronic obstructive pulmonary disease. *Thorax* **57**, 847–852 (2002).
11. Biswal, S., Thimmulappa, R. K. & Harvey, C. J. Experimental therapeutics of Nrf2 as a target for prevention of bacterial exacerbations in COPD. *Proceedings of the American Thoracic Society* **9**, 47–51, <https://doi.org/10.1513/pats.201201-009MS> (2012).
12. Seemungal, T. A. *et al.* Effect of exacerbation on quality of life in patients with chronic obstructive pulmonary disease. *American journal of respiratory and critical care medicine* **157**, 1418–1422, <https://doi.org/10.1164/ajrccm.157.5.9709032> (1998).
13. Sethi, S. & Murphy, T. F. Infection in the pathogenesis and course of chronic obstructive pulmonary disease. *The New England journal of medicine* **359**, 2355–2365, <https://doi.org/10.1056/NEJMra0800353> (2008).
14. Tanabe, N. *et al.* Impact of exacerbations on emphysema progression in chronic obstructive pulmonary disease. *American journal of respiratory and critical care medicine* **183**, 1653–1659, <https://doi.org/10.1164/rccm.201009-1535OC> (2011).
15. Brusselle, G. G., Joos, G. F. & Bracke, K. R. New insights into the immunology of chronic obstructive pulmonary disease. *Lancet* **378**, 1015–1026, [https://doi.org/10.1016/S0140-6736\(11\)60988-4](https://doi.org/10.1016/S0140-6736(11)60988-4) (2011).
16. Kang, M. J. *et al.* Cigarette smoke selectively enhances viral PAMP- and virus-induced pulmonary innate immune and remodeling responses in mice. *The Journal of clinical investigation* **118**, 2771–2784, <https://doi.org/10.1172/JCI32709> (2008).
17. Stampfli, M. R. & Anderson, G. P. How cigarette smoke skews immune responses to promote infection, lung disease and cancer. *Nature reviews. Immunology* **9**, 377–384, <https://doi.org/10.1038/nri2530> (2009).
18. D'Hulst, A. I., Vermaelen, K. Y., Brusselle, G. G., Joos, G. F. & Pauwels, R. A. Time course of cigarette smoke-induced pulmonary inflammation in mice. *The European respiratory journal* **26**, 204–213, <https://doi.org/10.1183/09031936.05.00095204> (2005).
19. Schindler, C. & Strehlow, I. Cytokines and STAT signaling. *Advances in pharmacology* **47**, 113–174 (2000).
20. Zheng, W. P. & Flavell, R. A. Pillars Article: The Transcription Factor GATA-3 Is Necessary and Sufficient for Th2 Cytokine Gene Expression in CD4 T Cells. *Cell* **1997**, 89: 587–596. *Journal of immunology* **196**, 4426–4435 (2016).
21. Yoshimura, A., Suzuki, M., Sakaguchi, R., Hanada, T. & Yasukawa, H. SOCS, Inflammation, and Autoimmunity. *Frontiers in immunology* **3**, 20, <https://doi.org/10.3389/fimmu.2012.00020> (2012).
22. Lee, S. H. *et al.* Antielastin autoimmunity in tobacco smoking-induced emphysema. *Nature medicine* **13**, 567–569, <https://doi.org/10.1038/nm1583> (2007).
23. van der Strate, B. W. *et al.* Cigarette smoke-induced emphysema: A role for the B cell? *American journal of respiratory and critical care medicine* **173**, 751–758, <https://doi.org/10.1164/rccm.200504-594OC> (2006).
24. Tsoumakidou, M., Demedts, I. K., Brusselle, G. G. & Jeffery, P. K. Dendritic cells in chronic obstructive pulmonary disease: new players in an old game. *American journal of respiratory and critical care medicine* **177**, 1180–1186, <https://doi.org/10.1164/rccm.200711-1727PP> (2008).
25. Sales, D. S. *et al.* Regulatory T-Cell Distribution within Lung Compartments in COPD. *Copd*, 1–10, <https://doi.org/10.1080/1541255.2017.1346069> (2017).
26. Chu, S. *et al.* The expression of Foxp3 and ROR gamma t in lung tissues from normal smokers and chronic obstructive pulmonary disease patients. *International immunopharmacology* **11**, 1780–1788, <https://doi.org/10.1016/j.intimp.2011.06.010> (2011).
27. Roos, A. B. *et al.* IL-17A and the Promotion of Neutrophilia in Acute Exacerbation of Chronic Obstructive Pulmonary Disease. *American journal of respiratory and critical care medicine* **192**, 428–437, <https://doi.org/10.1164/rccm.201409-1689OC> (2015).
28. Hasday, J. D., Bascom, R., Costa, J. J., Fitzgerald, T. & Dubin, W. Bacterial endotoxin is an active component of cigarette smoke. *Chest* **115**, 829–835 (1999).
29. Larsson, L., Szponar, B. & Pehrson, C. Tobacco smoking increases dramatically air concentrations of endotoxin. *Indoor air* **14**, 421–424, <https://doi.org/10.1111/j.1600-0668.2004.00290.x> (2004).
30. Sebastian, A., Pehrson, C. & Larsson, L. Elevated concentrations of endotoxin in indoor air due to cigarette smoking. *Journal of environmental monitoring: JEM* **8**, 519–522, <https://doi.org/10.1039/b600706f> (2006).
31. Sajjan, U. *et al.* Elastase- and LPS-exposed mice display altered responses to rhinovirus infection. *American journal of physiology. Lung cellular and molecular physiology* **297**, L931–944, <https://doi.org/10.1152/ajplung.00150.2009> (2009).
32. Kobayashi, S. *et al.* A single dose of lipopolysaccharide into mice with emphysema mimics human chronic obstructive pulmonary disease exacerbation as assessed by micro-computed tomography. *American journal of respiratory cell and molecular biology* **49**, 971–977, <https://doi.org/10.1165/rcmb.2013-0074OC> (2013).
33. Vernooy, J. H., Dentener, M. A., van Suylen, R. J., Buurman, W. A. & Wouters, E. F. Long-term intratracheal lipopolysaccharide exposure in mice results in chronic lung inflammation and persistent pathology. *American journal of respiratory cell and molecular biology* **26**, 152–159, <https://doi.org/10.1165/ajrcmb.26.1.4652> (2002).
34. Toledo, A. C. *et al.* Aerobic exercise attenuates pulmonary injury induced by exposure to cigarette smoke. *The European respiratory journal* **39**, 254–264, <https://doi.org/10.1183/09031936.00003411> (2012).
35. Ramos, D. S. *et al.* Low-intensity swimming training partially inhibits lipopolysaccharide-induced acute lung injury. *Medicine and science in sports and exercise* **42**, 113–119, <https://doi.org/10.1249/MSS.0b013e3181ad1c72> (2010).
36. Margraf, L. R., Tomashefski, J. F. Jr., Bruce, M. C. & Dahms, B. B. Morphometric analysis of the lung in bronchopulmonary dysplasia. *The American review of respiratory disease* **143**, 391–400, <https://doi.org/10.1164/ajrccm/143.2.391> (1991).
37. Evans, M. J., Cox, R. A., Shami, S. G., Wilson, B. & Plopper, C. G. The role of basal cells in attachment of columnar cells to the basal lamina of the trachea. *American journal of respiratory cell and molecular biology* **1**, 463–469, <https://doi.org/10.1165/ajrcmb/1.6.463> (1989).
38. Papi, A., Luppi, F., Franco, F. & Fabbri, L. M. Pathophysiology of exacerbations of chronic obstructive pulmonary disease. *Proceedings of the American Thoracic Society* **3**, 245–251, <https://doi.org/10.1513/pats.200512-1255F> (2006).
39. Makris, D. *et al.* Tc2 response at the onset of COPD exacerbations. *Chest* **134**, 483–488, <https://doi.org/10.1378/chest.07-2626> (2008).
40. Stefanska, A. M. & Walsh, P. T. Chronic obstructive pulmonary disease: evidence for an autoimmune component. *Cellular & molecular immunology* **6**, 81–86, <https://doi.org/10.1038/cmi.2009.11> (2009).

41. De Filippo, K., Henderson, R. B., Laschinger, M. & Hogg, N. Neutrophil chemokines KC and macrophage-inflammatory protein-2 are newly synthesized by tissue macrophages using distinct TLR signaling pathways. *Journal of immunology* **180**, 4308–4315 (2008).
42. Lee, J. *et al.* Chemokine binding and activities mediated by the mouse IL-8 receptor. *Journal of immunology* **155**, 2158–2164 (1995).
43. Chin, C. L. *et al.* Haemophilus influenzae from patients with chronic obstructive pulmonary disease exacerbation induce more inflammation than colonizers. *American journal of respiratory and critical care medicine* **172**, 85–91, <https://doi.org/10.1164/rccm.200412-1687OC> (2005).
44. Tanino, M. *et al.* Increased levels of interleukin-8 in BAL fluid from smokers susceptible to pulmonary emphysema. *Thorax* **57**, 405–411 (2002).
45. O'Donnell, R. A. *et al.* Relationship between peripheral airway dysfunction, airway obstruction, and neutrophilic inflammation in COPD. *Thorax* **59**, 837–842, <https://doi.org/10.1136/thx.2003.019349> (2004).
46. Fuke, S. *et al.* Chemokines in bronchiolar epithelium in the development of chronic obstructive pulmonary disease. *American journal of respiratory cell and molecular biology* **31**, 405–412, <https://doi.org/10.1165/rcmb.2004-0131OC> (2004).
47. Hardaker, E. L. *et al.* Exposing rodents to a combination of tobacco smoke and lipopolysaccharide results in an exaggerated inflammatory response in the lung. *British journal of pharmacology* **160**, 1985–1996, <https://doi.org/10.1111/j.1476-5381.2010.00857.x> (2010).
48. Saetta, M. *et al.* CD8+ve cells in the lungs of smokers with chronic obstructive pulmonary disease. *American journal of respiratory and critical care medicine* **160**, 711–717, <https://doi.org/10.1164/ajrccm.160.2.9812020> (1999).
49. Freeman, C. M. *et al.* Cytotoxic potential of lung CD8(+) T cells increases with chronic obstructive pulmonary disease severity and with *in vitro* stimulation by IL-18 or IL-15. *Journal of immunology* **184**, 6504–6513, <https://doi.org/10.4049/jimmunol.1000006> (2010).
50. Di Stefano, A. *et al.* T helper type 17-related cytokine expression is increased in the bronchial mucosa of stable chronic obstructive pulmonary disease patients. *Clinical and experimental immunology* **157**, 316–324, <https://doi.org/10.1111/j.1365-2249.2009.03965.x> (2009).
51. Zhang, J. *et al.* Increased expression of CD4+IL-17+ cells in the lung tissue of patients with stable chronic obstructive pulmonary disease (COPD) and smokers. *International immunopharmacology* **15**, 58–66, <https://doi.org/10.1016/j.intimp.2012.10.018> (2013).
52. Lane, N., Robins, R. A., Corne, J. & Fairclough, L. Regulation in chronic obstructive pulmonary disease: the role of regulatory T-cells and Th17 cells. *Clinical science* **119**, 75–86, <https://doi.org/10.1042/CS20100033> (2010).
53. Yew-Booth, L. *et al.* JAK-STAT pathway activation in COPD. *The European respiratory journal* **46**, 843–5, <https://doi.org/10.1183/09031936.00228414> (2015).
54. Vieira, P. L. *et al.* IL-10-secreting regulatory T cells do not express Foxp3 but have comparable regulatory function to naturally occurring CD4+CD25+ regulatory T cells. *Journal of immunology* **172**, 5986–5993 (2004).
55. Couper, K. N., Blount, D. G. & Riley, E. M. IL-10: the master regulator of immunity to infection. *Journal of immunology* **180**, 5771–5777 (2008).
56. Suvas, S., Azkur, A. K., Kim, B. S., Kumaraguru, U. & Rouse, B. T. CD4+CD25+ regulatory T cells control the severity of viral immunoinflammatory lesions. *Journal of immunology* **172**, 4123–4132 (2004).
57. Groux, H. *et al.* A transgenic model to analyze the immunoregulatory role of IL-10 secreted by antigen-presenting cells. *Journal of immunology* **162**, 1723–1729 (1999).
58. Netea, M. G. *et al.* Toll-like receptor 2 suppresses immunity against *Candida albicans* through induction of IL-10 and regulatory T cells. *Journal of immunology* **172**, 3712–3718 (2004).
59. Kullberg, M. C. *et al.* Bacteria-triggered CD4(+) T regulatory cells suppress *Helicobacter hepaticus*-induced colitis. *The Journal of experimental medicine* **196**, 505–515 (2002).
60. Anderson, C. F., Oukka, M., Kuchroo, V. J. & Sacks, D. CD4(+)-CD25(-)Foxp3(-) Th1 cells are the source of IL-10-mediated immune suppression in chronic cutaneous leishmaniasis. *The Journal of experimental medicine* **204**, 285–297, <https://doi.org/10.1084/jem.20061886> (2007).
61. Jin, Y. *et al.* Treg/IL-17 ratio and Treg differentiation in patients with COPD. *PloS one* **9**, e111044, <https://doi.org/10.1371/journal.pone.0111044> (2014).

Acknowledgements

Profa Carla Máximo Prado for LPS providing; Angela Santos and Esmeralda Eher for teaching immunohistochemistry techniques; Marcos Begnami for scanning the lung tissue samples. This research was supported by Coordenação de Aperfeiçoamento de Pessoal de Nível Superior (CAPES) and the Instituto dos Laboratórios de Investigação Médica do Hospital das Clínicas da Faculdade de Medicina da Universidade de São Paulo, Brazil (LIM - 20 - HC/FMUSP). This study also received the support from Sao Paulo Research Foundation (FAPESP), grant 2012/15165-2.

Author Contributions

D.A.B.C. performed the study design, performed all experiments, analyzed data, interpreted results of experiments, prepared figures, drafted manuscript, edited and revised manuscript; J.T.I. performed experiments: exposure to C.S.; animal euthanasia to remove lungs, immunohistochemistry and drafted manuscript; J.D.L. performed animals euthanasia to remove lungs; C.R.O. performed animals euthanasia to remove lungs; B.M.S.R. performed the B.A.L. experiment; R.A.V. performed the double immunostaining experiments and capture the double immunostaining photomicrographs; M.C.O.J. performed ELISA analysis; T.M. edited and revised manuscript; M.A.M. analyzed data, interpreted results of experiments, edited and revised manuscript; I.F.L.C.T. analyzed data, interpreted results of experiments, edited and revised manuscript; R.P.V. edited and revised manuscript; F.D.T.Q.S.L. performed the study design, performed experiments, analyzed data and edited and revised manuscript. All authors approved the final version of the manuscript.

Additional Information

Competing Interests: The authors declare no competing interests.

Publisher's note: Springer Nature remains neutral with regard to jurisdictional claims in published maps and institutional affiliations.



Open Access This article is licensed under a Creative Commons Attribution 4.0 International License, which permits use, sharing, adaptation, distribution and reproduction in any medium or format, as long as you give appropriate credit to the original author(s) and the source, provide a link to the Creative Commons license, and indicate if changes were made. The images or other third party material in this article are included in the article's Creative Commons license, unless indicated otherwise in a credit line to the material. If material is not included in the article's Creative Commons license and your intended use is not permitted by statutory regulation or exceeds the permitted use, you will need to obtain permission directly from the copyright holder. To view a copy of this license, visit <http://creativecommons.org/licenses/by/4.0/>.

© The Author(s) 2019